Curing of Composites by Radiation and Natural Convection in an Autoclave

P. Salagnac, P. Dutournié, and P. Glouannec
Laboratoire d'Etudes Thermiques, Energétiques et Environnement (LET2E), Université de Bretagne-Sud, Centre de recherche, 56321 Lorient Cedex, France

DOI 10.1002/aic.10224
Published online in Wiley InterScience (www.interscience.wiley.com).

As a major objective, the feasibility is checked of the curing of composite material parts in a small diameter autoclave. The material must respect a temperature cycle curing and different thermal constraints. The particularity of this study is the heat exchanges which are mainly free convection and radiation. The temperature profile and the reticulation conversion yield are determined in a section of the autoclave by numerical simulations at different functioning pressures and commented. An experimental investigation has been made at atmospheric pressure. The measured data well agreed with the simulated results. This study allows us to validate this autoclave designed for the curing of composite material parts. © 2004 American Institute of Chemical Engineers *AIChE J,* 50: 3149–3159, 2004
Keywords: autoclave, curing, composite material, thermal modeling, experiment

Introduction

This article reports the process followed in the design of a small-diameter autoclave intended for curing material composite parts. The autoclave process is one of the most common techniques used for manufacturing composite materials such as in the naval, automobile, and aeronautic industries. In principle, composite preimpregnated (prepregs) woven fiber mats impregnated with resin are used. First, they are cut and assembled in the shape of the part. Then, the laminate is placed on a mold, bagged, and introduced into the autoclave before the curing process. A cure cycle is selected to obtain high-performance materials. The optimization of thermal conditions and autoclave designed for production of composite materials is an active field of development and research in numerous industries (Antonucci et al., 2002; LeGrand and Bellenger, 1998; Li et al., 2001; Olivier and Cottu, 1998). Most studies primarily aim at reducing capital and energy requirements and improving the quality of products.

The purpose of this work is the feasibility study of a small-diameter autoclave for the curing of composite materials, which for this study come from the naval industry. They have small sections and can be very long (many meters). In the classical processes, the heats between matrix and air are exchanged by forced convection (Antonucci et al., 2001; Oh and Lee, 2002). The particularity of this study arises from the heat exchanges, which are mainly free convection and radiation. Different constraints should be taken into account. To obtain final products of good quality, one must first respect the curing temperature cycle. Next, the thermal gradients in the curing parts must be as small as possible. Then, the temperatures of the composite matrix and the tubular steel must be less than 135 and 300°C, respectively.

The aim of this work was to determine the temperature distribution and the conversion yield in a section of the autoclave by numerical simulations, using a computational fluid dynamic (CFD) code (FLUENT, Lebanon, NH). Then, numerical results are validated by experiments. The heat exchanges between the tubular steel and the bag–composite–tool element activate and allow control of the exothermic curing reactions. By taking into account the different heat exchanges (conduction, convection, and radiation) with the internal heat contribution (reticulation reaction) we can heighten our knowledge of the temperature distribution in the materials during the curing process. First, the physical model and its implementation are presented. A dimensionless analysis is carried out to identify the significant parameters and variables, and a numerical simulation at 0.6 MPa is shown.

Correspondence concerning this article should be addressed to P. Salagnac at patrick.salagnac@univ-ubs.fr.

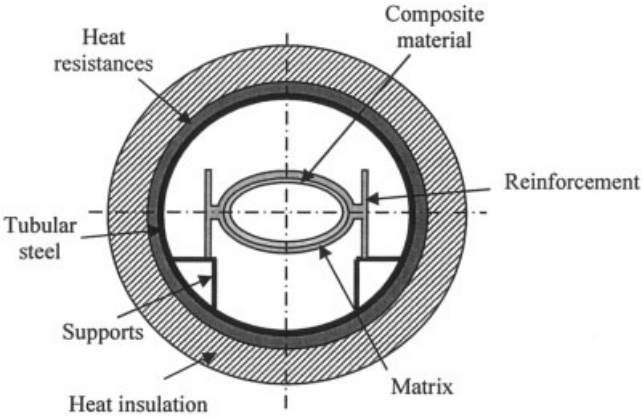

Figure 1. Cross section of the autoclave.

The second part of this report describes numerical and experimental studies carried out at 0.1 MPa. A curing pilot has been made with a geometry and a heat system similar to that of the autoclave. Tests conducted on carbon/epoxy material are presented.

Thermal Modeling

Autoclave description

The autoclave is a cylindrical steel reactor, the inner diameter of which is 40 cm (Figure 1). Its outer side is heated by electrical resistances. The autoclave is wrapped with an insulated material. In the reactor, the composite material to be cured is placed in a matrix designed for long parts. The matrix has two lateral reinforcements (53 mass % of the matrix mass) to be placed on supports, as described in Figure 1. This reactor can operate at atmospheric pressures up to 0.6 MPa.

Because the reactor diameter is small compared to the autoclave length, a two-dimensional (2-D) model can be used to describe the heat and mass transfer process. The study is carried out for symmetric materials with respect to the vertical axis.

In this case, the heat transport is attributed to free convection and radiation in fluid and pure conduction in solid. In practice, the molded part is inserted into the matrix at vacuum pressure, which improves the contact between the matrix and the molded part. Thus, the thermal contact resistances between the following layers of materials are neglected. During the curing process, an irreversible chemical reaction, called *reticulation*, is set in motion; this reaction produces heat (Bailleul et al. 1996; Sun et al., 2002).

Governing equations

The two-dimensional unsteady-state governing equations for a classical compressible laminar fluid in a Cartesian coordinate system, indicated with subscripts (1, 2), may be written as (FLUENT, 2001; Park et al., 2003):

Continuity Equation. For $i = 1, 2$:

$$\frac{\partial \rho}{\partial t} + \frac{\partial (\rho u_i)}{\partial x_i} = 0 \tag{1}$$

Navier–Stokes Equations. For $i, j, k = 1, 2$:

$$\frac{\partial (\rho u_i)}{\partial t} + \frac{\partial (\rho u_i u_j)}{\partial x_j} = \frac{\partial}{\partial x_j}\left[\mu\left(\frac{\partial u_i}{\partial x_j} + \frac{\partial u_j}{\partial x_i}\right) - \frac{2\mu}{3}\frac{\partial u_k}{\partial x_k}\delta_{i,j}\right] - \frac{\partial p}{\partial x_i} + \rho g_i \tag{2}$$

Energy Equation. For $i = 1, 2$:

$$\frac{\partial (\rho E)}{\partial t} + \frac{\partial [u_i(\rho E + p)]}{\partial x_i} = \frac{\partial}{\partial x_i}\left(\lambda \frac{\partial T}{\partial x_i}\right) \tag{3}$$

The energy equation for solids, for $i = 1, 2$, is

$$\frac{\partial (\rho h)}{\partial t} = \frac{\partial}{\partial x_i}\left(\lambda \frac{\partial T}{\partial x_i}\right) + S_\alpha + S_h \tag{4}$$

where S_h is the radiation source term and S_α includes heat production of the chemical reaction. This last term is necessary only for the molded part. The heat of chemical reaction is written as (Bailleul et al. 1996)

$$S_\alpha = \rho \Delta h^r \frac{\partial \alpha}{\partial t} \tag{5}$$

The radiative transfer equation for an absorbing, emitting, and scattering medium at position $\vec{r}$ in the direction $\vec{s}$ is written as

$$\frac{dI(\vec{r}, \vec{s})}{ds} + (a + \sigma_s) I(\vec{r}, \vec{s}) = an^2 \frac{\sigma T^4}{\pi} + \frac{\sigma_s}{4\pi}\int_0^{4\pi} I(\vec{r}, \vec{s}\,')\Phi(\vec{s} \cdot \vec{s}\,')d\Omega' \tag{6}$$

where $\vec{s}\,'$ is the scattering direction vector.

At the selected pressure, the thermophysical properties of air are assumed as polynomial functions of temperature and air is assumed as a transparent medium. The density, the specific heat, and the thermal conductivity of the tubular steel are constant. Moreover, it is assimilated to a gray body with diffuse emission and reflection.

Boundary and initial conditions

The velocity is set to zero at the walls. All the perpendicular gradients (temperature, conversion yield, velocity, and pressure) are null on the vertical symmetric axis. The tubular steel temperature varies as a function of time. The temperature distribution inside the autoclave is initially uniform and at room temperature.

Dimensionless analysis

As an aid in better understanding the phenomena and to identify the significant parameters and variables, a nondimensional analysis is carried out in the matrix and the curing

Table 1. Dimensionless Parameters at Different Positions and Different Times

Matrix						
Time (s)	3000		4000		4500	
Location	Lower	Upper	Lower	Upper	Lower	Upper
T_{matrix} (°C)	111.9	105.9	124	116.9	131.4	135.9
h_r (W m^{-2} K^{-1})	6.3	6.1	7.1	6.5	7.2	7.4
h_c (W m^{-2} K^{-1})	34.5	12.0	40.0	1.7	12.9	15.5
Bi radial	0.40	0.18	0.46	0.08	0.20	0.22
t_c (s) radial			142			
t_c (s) orthoradial			24,282			

Curing Part									
Time (s)	3000			4000			4500		
Location	Lower	Middle	Upper	Lower	Middle	Upper	Lower	Middle	Upper
$T_{curing\ part}$ (°C)	103.5	98.7	95.3	133.4	120.6	112.3	144.6	141.5	137.1
t_r (s)	2399	3337	4221	373	800	134.6	204	237	302
Da radial	0.018	0.013	0.010	0.114	0.053	0.32	0.209	0.181	0.142
Da orthoradial	4.4	3.2	2.5	28.2	13.2	7.8	51.7	44.5	34.9
t_c (s) radial					36				
t_c (s) orthoradial					8740				

composite part. The dimensionless variables are defined as (Antonucci et al., 2001; Li et al., 2001)

$$t^+ = \frac{t}{t_c} \qquad \eta^+ = \frac{\eta}{L} \qquad \tau^+ = \frac{\tau}{L}$$

$$\theta = \frac{T - T_0}{\Delta T_c} \qquad \text{with } \Delta T_c = T_\infty - T_0$$

where (η, τ) are the normal and tangential coordinates and L is the characteristic dimension of the matrix in the chosen direction.

The dimensionless form of the energy equation for the matrix is

$$\frac{\partial \theta}{\partial t^+} = \frac{\lambda t_c}{\rho C_p L^2} \Delta^+ \theta \tag{7}$$

where Δ^+ is the dimensionless Laplacian operator in the coordinates system (η^+, t^+) and $t_c = \rho C_p L^2/\lambda$.

At the contact between matrix and composite material, the dimensionless boundary condition is

$$\frac{\partial \theta}{\partial \eta^+} = \frac{\lambda_{cm}}{\lambda} \frac{\partial \theta_{cm}}{\partial \eta^+} \tag{8}$$

At the contact between matrix and air, we have

$$\frac{\partial \theta}{\partial \eta^+} = \frac{h_c L}{\lambda} (\theta_{air} - \theta) + \frac{h_r L}{\lambda} (\theta_{tubular} - \theta) \tag{9}$$

Four dimensionless numbers are used in these equations. Fo $= (\lambda t_c)/(\rho C_p L^2)$ is the Fourier number and provides the penetration of a thermal perturbation during the time t_c. $\lambda_{cm}/\lambda = 0.54$ is the ratio of thermal conductivity (composite material/matrix). $\mathrm{Bi}_c = h_c L/\lambda$ and $\mathrm{Bi}_r = h_r L/\lambda$ are the Biot numbers for convective and radiative heat transfer, respectively. They represent the ratio of conductive thermal resistance on the convective or radiative thermal resistance.

The Biot number (convection) takes different values at different positions (Table 1). The convective heat exchange coefficient varies substantially with the complex geometry of the matrix and the fluid temperature. In opposition to processes working in forced convection, this fluid temperature in the autoclave is not homogeneous. Moreover, the Biot number (radiation) depends significantly on the geometry. The two lateral reinforcements change the view factor. The boundary condition at the external area is inhomogeneous, and thus it is not possible to neglect heat transfers in the tangential direction.

A simple calculation shows that the two Biot numbers are of the same order. The use of basic correlations (Bayazitoglu and Özisik, 1988) to determine convective and radiative heat transfer coefficients indicates that the values are in the range of 1 to 40 W m^{-2} K^{-1}. These values give Biot numbers in the normal direction included between 0.06 and 0.5, respectively. Neither the normal conduction nor the tangential conduction can be neglected.

For the dimensionless form of the energy equation for the curing material part, other dimensionless variables are defined as follows

$$\Delta T_a = \frac{\Delta h^r}{C_p} \qquad t_r = k_{ref}^{-1} \exp\left(\frac{A}{T}\right)$$

where ΔT_a denotes the adiabatic temperature increase of the curing material, t_r is the characteristic time for reaction at dimensionless temperature θ_{cm}, and L is the characteristic dimension of the curing material in the chosen direction

$$\frac{\partial \theta_{cm}}{\partial t^+} = \frac{\lambda_{cm} t_c}{\rho_{cm} C_{p,cm} L^2} \Delta^+ \theta_{cm} + \frac{\Delta T_a}{\Delta T_c} \left(\frac{t_c}{t_r}\right) G(\alpha) \tag{10}$$

where $G(\alpha)$ is a first-order dimensionless cure kinetic function.

At the contact between matrix and composite material, the

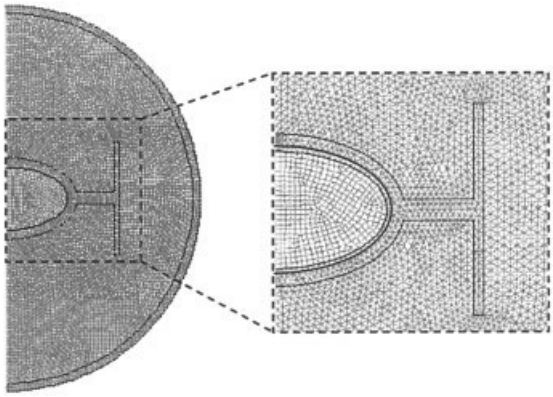

Figure 2. Computational domain and grid.

dimensionless boundary condition is represented by Eq. 8. At the contact between composite material and interior air, we have exchanges by convection and radiation smaller than those of the matrix (Eq. 9). The quantity t_c/t_r represents the ratio of the diffusion to reaction timescales (Table 1). This ratio is always <1 in the radial direction and always >1 in the tangential direction. The degree of cure will be uniform inside the composite part if the composite temperature has been uniform. In our case, there are thermal gradients in the curing material. Therefore, the degree of cure is nonuniform. The Damköhler number, $\mathrm{Da} = (\Delta T_d/\Delta T_c)(t_c/t_r)$, is a ratio of the rate of temperature change caused by reaction to the rate of temperature change caused by conduction. It is <1 in the thickness of the curing part and >1 in the tangential direction. (Because the boundary conditions are not homogeneous, the conduction time cannot be the same in the tangential direction. In fact, the characteristic length is a function of the boundary conditions $L_\tau \gg L_\eta$.) This induces a gradient of the degree of cure in the material.

To summarize this dimensionless analysis, the heat contributions by free convection and radiation are of the same order. The complexity of the geometry and the different heat contributions do not permit us to attempt a one-dimensional, time-dependent solution in the thickness direction.

Simulation Results at 0.6 MPa

Numerical solution procedure

The geometry, the boundary conditions, and the heat and mass transfers are symmetrical with respect to the vertical axis. Therefore, only half of the autoclave was studied (Figure 2). To solve the partial differential equations previously described (Eqs. 1–6), the domain (Figure 1) was discretized with an unstructured grid of about 13,000 finite elements (Figure 2) with Gambit 2.0. The FLUENT software package (version 5.5) with the segregated solver was used. The numerical procedure is explained in a block diagram (Figure 3). The radiative transfer equation is solved with a discrete ordinates (DO) radiation model (Chui and Raithby, 1993). Continuity and momentum balances are coupled by the SIMPLE algorithm (Patankar, 1980), a standard scheme is used for the pressure discretization, and a first-order upwind is used in the momentum and energy equations. The implicit formulation is used. Values of 10^{-3} were used as the convergence criteria at each time step for the sum of each normalized residual over the

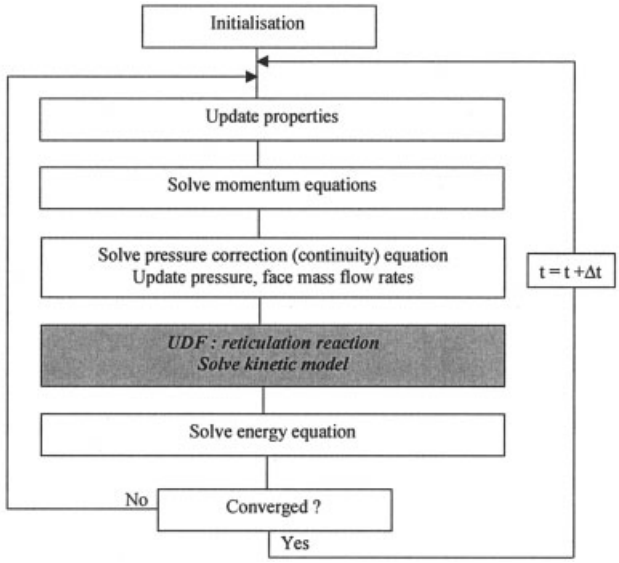

Figure 3. Block diagram of numerical procedure.

whole fluid domain for all governing fluid flow equations (continuity and velocities). A convergence criterion of 10^{-7} in energy and DO intensity was selected.

The reaction kinetic and the heat generated by the reticulation are implemented in FLUENT as user-defined functions (UDF) in the C programming language. This UDF is interpreted during solver execution.

Tested materials

To test the autoclave feasibility, a molded part in carbon/epoxy (4 mm thick) and a matrix in glass/epoxy (6 mm thick) were chosen.

Thermophysical Properties. The composite materials properties depend on the mass fraction of each component, presented in Table 2. The thermal conductivity is calculated with the Springer–Tsaï model (Bailleul, 1997), using the intrinsic thermal conductivity values of each main component. The heat capacity is obtained with an additive model by adding the thermal contribution of each pure component. The density is calculated with a series model from mass fractions.

Reaction Heat. The difficulty during the thermal processing is to take into account and quantify this heat source. Many works are devoted to the study of reticulation reaction (for example, Bailleul, 1997; Nzihou et al., 1999; Um et al., 2002). Several curing experiments have been conducted to estimate the reaction heat. Some samples (carbon/epoxy) have been cured in a differential scanning calorimeter (Perkin–Elmer DSC Pyris 1) at different heating rates (0.5–10°C/min). An empty cycle is subtracted from each cycle to eliminate the

Table 2. Properties of Composite Materials

Property	Carbon/Epoxy	Glass/Epoxy
Mass fraction	62%/38%	60%/40%
Density, kg m^{-3}	1490	1772
Thermal conductivity, W m^{-1} K^{-1}	0.65	0.35
Specific heat, J kg^{-1} K^{-1}	876	880
Emissivity		0.5

Table 3. Experimental Determination of Reaction Heat for Different Heating Rates

Test	Heating Rate (°C/min)	Reaction Heat (kJ kg^{-1})
1	0.5	125.1
2	1	87.7
3	1.5	109.4
4	2	107.1
5	3	101.2
6	5	110.7
7	7	103.4
8	10	107.7

influence of perturbations (heat losses) and to take into account the specific heat variations. These experimental results give the reaction enthalpies as functions of time or temperature. Overall reaction enthalpy is determined by integration of the exothermal peak (see Table 3).

Thus, the average reaction heat of this carbon/epoxy material was estimated as $\Delta h^r = 106.1$ kJ kg^{-1}. This energy represents the heat of the 38% of epoxy contained in the curing material.

Kinetic Modeling. With the same experiments, the reaction rates $\partial\alpha/\partial t$ are calculated by the partial integration of the experimental curves, as follows

$$\frac{\partial \alpha}{\partial t} = \frac{\int_0^t \frac{dh^*}{dt}\, dt}{\int_0^\infty \frac{dh^*}{dt}\, dt} \tag{11}$$

where h^* is the enthalpy of the material corrected with respect to the specific heats and heat losses in the system. These results have shown that reactions rates depend on both temperature and conversion yield.

Reaction rates vs. conversion yields were plotted for different temperatures. For all curves, the maxima of reaction rates are obtained at the same conversion yield ($\alpha = 0.27$). Thus we have constructed the hypothesis of variable separation for the kinetic law.

From these considerations, the model (Eq. 12) chosen to describe the kinetic reaction is that developed by Bailleul (1997)

$$\frac{\partial \alpha}{\partial t} = K(T)G(\alpha) \tag{12}$$

where $K(T)$ is an Arrhenius law

$$K(T) = k_{ref}\exp\left[-\frac{A}{T}\right] \tag{13}$$

and $G(\alpha)$ is a polynomial formulation

$$G(\alpha) = \sum_{i=0}^{n} b_i \alpha^i \tag{14}$$

The process used to access the different constants (k_{ref}, A, b_i) is the same as that described in the literature (Bailleul, 1997). Values of these constants are presented in the notation section. The maximum of the G function was calculated as 1. Maximum points of the G function are used to determine the K function. k_{ref} and A are obtained by the plot

$$\ln(K) = f\left(\frac{1}{T}\right) \tag{15}$$

Determination of the G function was obtained by a residuals minimization (according to the meaning of least squares).

Figure 4 presents the numerical calculation of the kinetic vs. temperature. These curves were calculated for five different heating rates and they are compared to the experimental data. We note a good agreement between experimental and calculated kinetics, and thus the kinetic modeling can be validated.

Discussion

To illustrate this work, simulation results obtained at 0.6 MPa are presented. Several numerical experiments were carried out to determinate the temperature of the tubular steel and to obtain an adapted curing cycle: at the beginning, the tem-

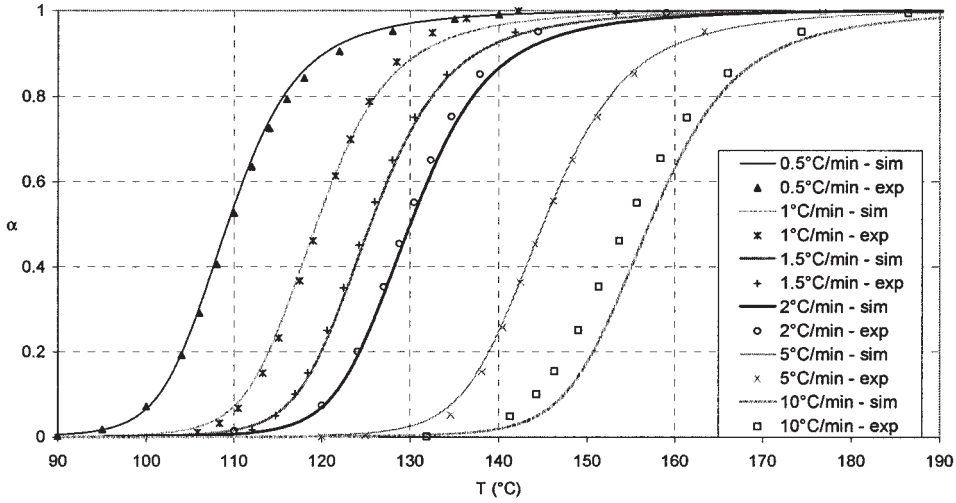

Figure 4. Experimental and calculated conversion yield vs. temperature for different heating rates.

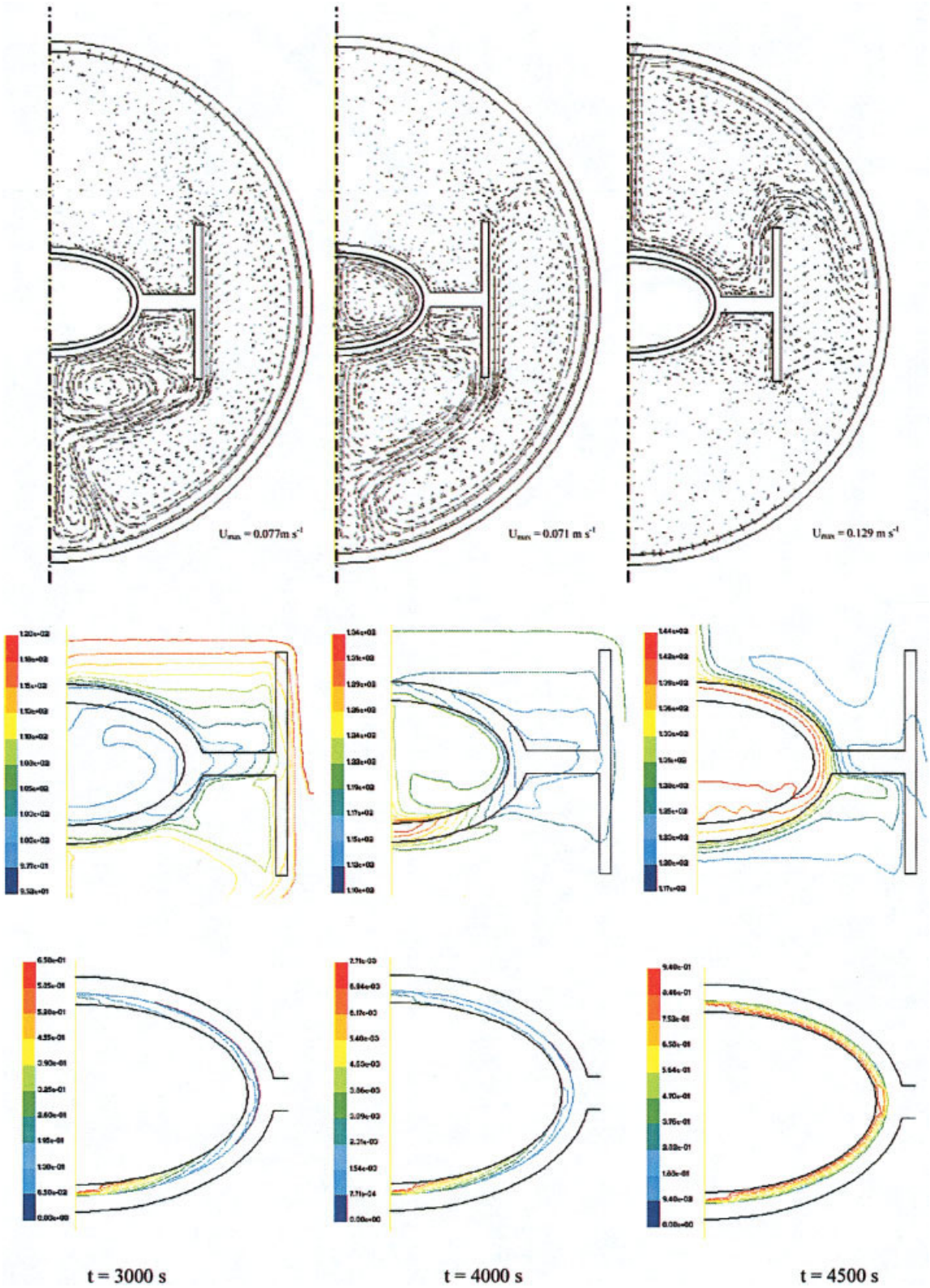

Figure 5. Velocity vectors, temperature contours, and conversion yield in the reactor at t = 3000, 4000, and 4500 s.

perature is 60°C and it increases linearly to 120°C over a period of 1750 s. After this heating rate, the temperature of the tubular steel is maintained at 120°C.

Figure 5 shows the velocity vectors, temperature, and conversion yield contours before start of the reaction and both during and after the reaction. By 3000 s after start of the system, the velocity profiles present several recirculations in the lower part of the reactor, where temperatures are included

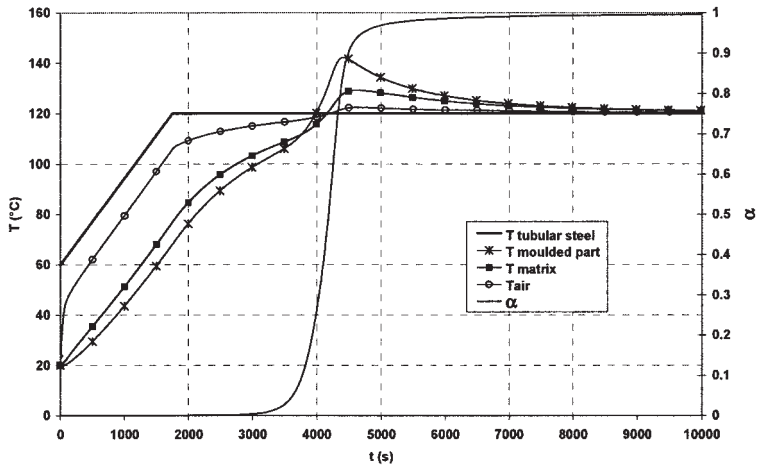

Figure 6. Tubular steel, molded part, matrix, and air average temperatures vs. time and conversion yield vs. time.

between 105 and 115°C. In the upper part, the velocity intensities are quasi-null (identical for the inner fluid, $T \approx$ constant = 95°C) except in the zone between the matrix and the support where the fluid temperature is stratified. The fluid temperature is around $T = 105$°C, close to that of the matrix (same temperature in the lower part of the matrix near the reinforcement). The temperature of the molded part is included between 95 and 105°C.

At $t = 4000$ s, the reaction has started. The velocity profiles are similar to those in the preceding case, except for the inner fluid, where there is a significant convective motion. The air temperature is more homogeneous than that in the previous case. In the molded part, there is a high temperature gradient as a result of the reaction. The lower segment of the molded part is at 134°C ($\alpha = 0.65$), whereas the upper part is at 126°C ($\alpha = 0.195$). The part adjacent to the reinforcement is at 110°C ($\alpha = 0.065$). The main effect of significant convective recirculation in the inner part of the reactor is to homogenize temperatures.

By 4500 s after start of the system, the reaction is quasi-completed (average conversion yield: 0.94) and the temperature of the molded part is more homogeneous than previously. The principal difference with the preceding cases is that the velocity profiles have been completely changed. Now, the recirculation zones are placed in the upper part of the fluid (hot zone: 120–134°C) and the lower part is a cold zone without recirculation (120°C). Only a small recirculation is in the lower part of the reactor located between the matrix and the reinforcement. This convective movement cools down the molded part faster than in other parts ($T = 136$°C compared to 144°C for the rest of the material). After 5000 s, the material cooling continues with two recirculations between the matrix and the reinforcement in both the lower and the upper parts of the reactor. At this moment, the hot zones constitute the part near the symmetrical axis. Figure 6 shows the average temperature evolutions vs. time of tubular steel, molded part, matrix, and air. The second axis presents the evolution of the average conversion yield vs. time.

As expected, the matrix, the molded part, and air heating rates are uniform until $t = 3000$ s. At this time, thermal conditions are limited to the start of reaction. The heat generated by the reticulation reaction induces an increase of temperature in the molded part. From this moment, the temperature of the molded part becomes higher than that of the rest of the system. Then, matrix and air make use of the heat evacuation system. Around 5000 s after start of the reaction, reticulation is nearly completed, and the heat exchanges between molded part, matrix, tubular steel, and air make the entire temperature range uniform. The reaction generates a 22°C temperature

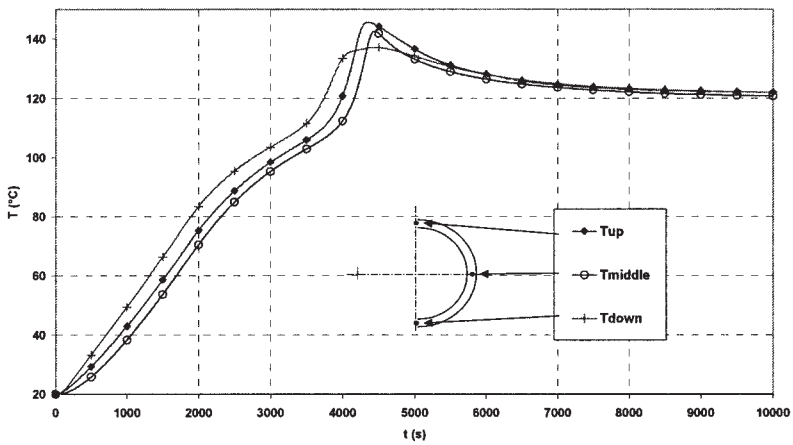

Figure 7. Evolution of molded part temperatures at different positions.

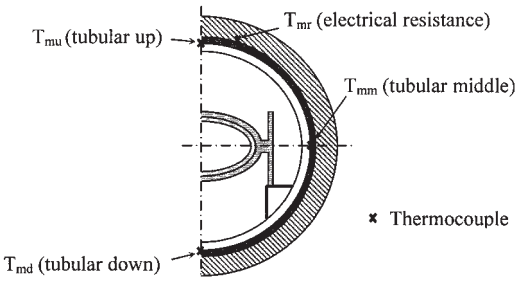

Figure 8. Positions of thermocouples on tubular steel in a middle cross section.

exceeding (average molded part temperature) that with respect to the imposed temperature (tubular steel). This maximum is reached around 4350 s after start of the system.

The highest temperature in the material is reached when the conversion yield is around 80–90%.

Figure 7 shows the evolution of temperature of the molded part at three different positions. We observe significant differences of temperature in the composite material according to the position. As observed (Figure 5), the temperature in the lower part is higher than both the upper and the middle temperatures. By 4000 s after start of the reaction, the reaction in the lower part is almost completed, after which the reaction begins at the middle position. The circumferential variation of temperature in the molded part cannot be neglected (the difference of temperature at 4000 s between the lower part and the middle part is around 20°C).

The minimization of temperature gradients in the molded part requires an increase of heat evacuation in the material. For this, an increase of conductive heat transfer between the molded part and the matrix is necessary.

The thermal behavior of this reaction is complex. The start of the reticulation reaction is a function of the velocity of temperature increasing in the material. The faster the increase of temperature, the higher the starting reaction temperature. Therefore, it is not possible to increase all heat transfers in the reactor because the starting temperature of the reaction also increases. Moreover, the maximum of temperature and the thermal gradients in the molded part will not decrease, despite the increase of all heat transfers.

Results of Simulations and Comparison with Experimental Data at 0.1 MPa

In this section, numerical simulation results obtained at 0.1 MPa are presented and compared with experimental test. To achieve this objective, we have designed an experimental pilot that works at atmospheric pressure and also allows testing of the heat elements.

Experimental apparatus

The design of the experimental furnace (length 1.2 m; inner diameter 40 cm) is nearly the same as that of the autoclave, presented previously.. For the heating system, electrical resistances are placed on the outer contour of the cylindrical steel reactor. The power of electrical resistances is regulated through two compact analogue thyristors working in phase angle and controlled with a PID (proportional integrative derivative) regulator.

Temperatures within the molded part, the matrix, and the tubular steel are recorded by thermocouples (type K, 0.5 mm in diameter) to determine the evolution of the system. The sensor positions in the middle of the furnace are described in Figure 8. Other thermocouples are placed on the length of the furnace (T_{eu}, "end-up") and on the electrical resistances.

The thermocouple T_{mr} feeds information to the regulator, which controls the electrical resistances. The whole experiment is monitored through a personal computer equipped with an analog–digital conversion board, which enables plotting of various measurements.

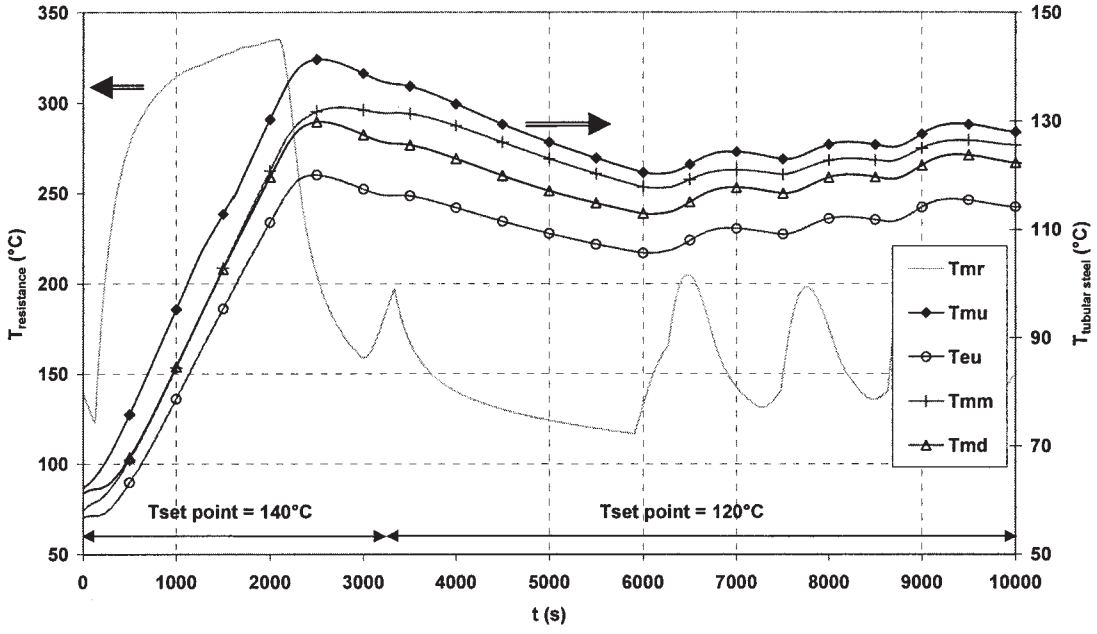

Figure 9. Tubular steel temperatures and resistance temperature vs. time (experimental results).

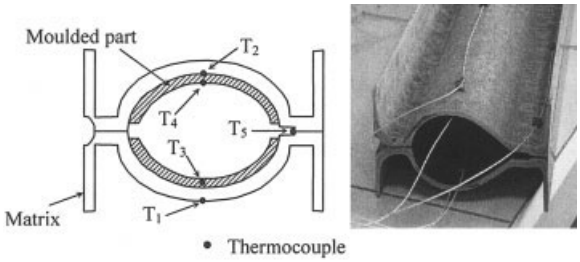

Figure 10. Positions of thermocouples in the molded part and the matrix/matrix picture.

Operating conditions

To have good mechanical characteristics in the curing material, a thermal procedure must be followed: the temperature of the molded part should increase linearly (1.5°C/min) and stabilize at 120°C. To obtain this cycle of temperature, the tubular steel temperature evolution must be determined beforehand. Different tests without and with matrix were carried out, but the more significant test is presented in Figure 9.

First, empty tubular steel was preheated at 60°C. When the molded part and the matrix are introduced into the furnace, the temperature of the proportional regulator is set at 140°C. The velocity of temperature increase of the wall is maximum. When the matrix temperature reaches 90°C (within about 2800 s), a set point temperature is imposed at 120°C to anticipate the matrix inertia and the reaction heat (Figure 9). This temperature of 90°C corresponds to the start of the reticulation reaction.

The maximum temperature (T_{mr}) of the electrical resistance (Figure 9) is around 330°C. Thus, the temperatures of the tubular steel at different positions are already below 300°C. This thermal limitation for a pressure apparatus is respected.

In Figure 9, thermal gradients can be observed in the middle section of the apparatus. In the same way, there is a significant difference of temperatures along the contour tubular steel of the pilot. These gradients are the consequence of boundary effects and poor homogeneity of the insulation. A maximum difference temperature obtained along the reactor length is about 22°C.

Experimental results and discussion

Figure 10 shows the positions of the different temperature measurements in the molded part and the matrix. The error of the temperature measurements is attributed to the incertitude of the system (thermocouples/instrumental equipment) (±2.5°C) and the problems of implantation in situ (2%).

Figure 11 presents the temperature evolutions vs. time during the curing process. The desired velocity of heating rate (1.5°C/min) is obtained, with a tubular steel temperature <150°C. The measurements at different positions in the part show no significant thermal gradients. The temperature evolutions for thermocouples 2 and 4 are very close with respect to the thickness. Around 100°C, the material temperature increases faster. In this temperature range, the reaction heat is maximum. This rapid increase of temperature generates overheating (127°C).

During the reaction, the temperature evolution at position 3 is in advance of the others (T_2, T_4) because it is located in the lower of the composite part. As observed in the simulations, the temperature increases faster in the lower part of the autoclave and thus the reaction starts first. By the end of the reaction, the temperatures converge to 120°C.

Simulation results and comparison

A first simulated test was carried out with an imposed tubular steel temperature: $T = (T_{mu} + T_{md})/2$. The numerical temperature profiles are close to the experimental results. However, the simulated increasing of temperature at the beginning of the curing process is faster than the experimental value. As a result, there is an earlier reaction start and a greater increase of temperatures of the matrix and molded part during the reaction. The average temperature at the end of the process is 5° higher than that in the experimental results.

To take into account the experimental boundary effects, the imposed temperature of the tubular steel was modified, which

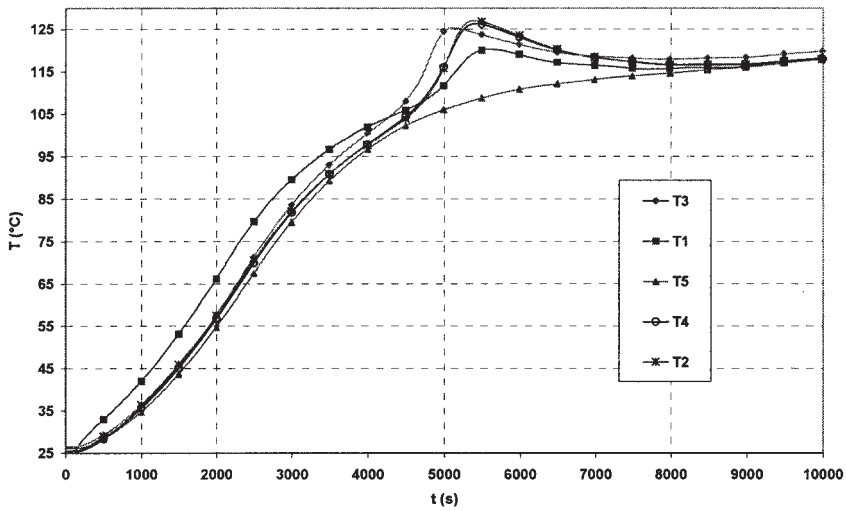

Figure 11. Evolutions of molded part temperature and matrix temperature vs. time (experimental results).

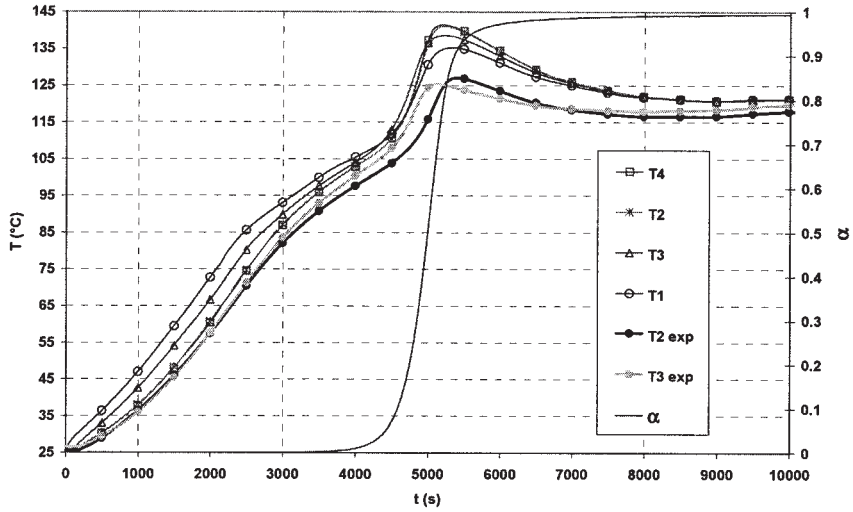

Figure 12. Evolutions of temperature profiles and average conversion yield vs. time (experimental and simulated results).

is an average of temperatures in the section subjected to the temperature near the end of the reactor: $T = T_{mu}/4 + T_{md}/4 + T_{eu}/2$.

Figure 12 shows the cure-induced temperature at points 1 to 4 marked in Figure 10 and the average degree of cure during the simulated process. These results are compared with experimental results (T_2 and T_3). As expected, the introduction of a new exterior tubular steel temperature modifies kinetic and heat transfers. The comparison of experimental and simulated data shows:

- The numerical heating rate is faster than the experimental one. As expected, the simulated reaction starts before the experimental one.
- The temperature maximum of the material part is higher (141°C) than the experimental temperature (127°C).

These results can be explained by a small difference of heating rate, which is the consequence of the approximation of the chosen tubular steel temperature. The end temperature substantially agrees with the experimental data (about 120°C).

Conclusion

In this report, we have presented a comparison between numerical simulations and experimental data of a curing process for carbon–epoxy material in a particular autoclave. A computer program was developed for the calculation of kinetics and included in a general software. The numerical model takes into account the convective, radiative heat transfers and reticulation reaction heat. The thermal behaviors of the curing part, matrix, and air were determined.

In spite of the differences of experimental temperature (tubular steel) along the reactor, the comparison between numerical and experimental cure processes shows a relatively good prediction of thermal behavior in the materials. The differences between simulations and experimental results are the consequence of the chosen tubular steel temperature. It has been shown that the present work can be used to examine and predict the thermal behavior of a composite material during a curing process at different static pressures. This numerical study, validated by experimental investigations, demonstrates the feasibility of this technology to cure small-diameter composite parts.

Acknowledgments

The authors gratefully acknowledge L. Tournier (Héol Composites) for suggesting this investigation.

Notation

a = absorption coefficient
g = body forces
E = energy
h = enthalpy
h^* = corrected enthalpy
h_c = convective heat transfer coefficient
h_r = radiative heat transfer coefficient
I = total radiation intensity
L = characteristic length
n = refractive index
p = static pressure
s = path length
S = heat source
t = time
t_c = characteristic time of conduction
t_r = characteristic time of the reaction
T = temperature
u = velocity components
U = mean velocity vector
x = spatial coordinates

Greek letters

α = conversion yield
Φ = phase function
σ = Stefan–Boltzmann constant
σ_s = scattering coefficient
Δh^r = heat of reaction
λ = thermal conductivity
μ = dynamic viscosity
Ω' = solid angle
ρ = density

Subscripts

ϕ = initial
∞ = final

cm = curing material

Coefficients for kinetic simulation

$k_{ref} = 40.703 \times 10^6\ s^{-1}$
$A = 9531.217$ K
$b_0 = 0.006$
$b_1 = 9.015$
$b_2 = -30.13$
$b_3 = 47.266$
$b_4 = -40.08$
$b_5 = 13.924$

Literature Cited

Antonucci, V., M. Giordano, K. T. Hsiao, and S. G. Advani, "A Methodology to Reduce Thermal Gradients due to the Exothermic Reactions in Composites Processing," *Int. J. Heat Mass Transfer*, **45**, 1675 (2002).

Antonucci, V., M. Giordano, S. I. Imparato, and L. Nicolais, "Analysis of Heat Transfer in Autoclave Technology," *Polym. Compos.*, **22**, 613 (2001).

Bailleul, J. L., "Optimisation du cycle de cuisson de pièces épaisses en matériau composite. Application à un imprégné résine époxyde/fibres de verre," PhD Thesis, University of Nantes, France (1997).

Bailleul, J. L., Y. Jarny, E. Artyukhin, and D. Delaunay, "Identification and Control of Heat Sources in Materials during Thermal Processing," *Inverse Problems Eng.*, **4**, 111 (1996).

Bayazitoglu, Y., and M. N. Özisik, *Elements of Heat Transfer*, McGraw-Hill, New York (1988).

Chui, E. H., and G. D. Raithby, "Computation of Radiant Heat Transfer on a Non-Orthogonal Mesh Using the Finite-Volume Method," *Numer. Heat Transfer B*, **23**, 269 (1993).

FLUENT Software, *User's Guide*, Fluent, Lebanon, NH (2001).

LeGrand, M., and V. Bellenger, "The Cure Optimisation of Carbon Epoxy Prepregs," *Compos. Sci. Technol.*, **58**, 639 (1998).

Li, M., Q. Zhu, P. H. Geubelle, and C. L. Tucker III, "Optimal Curing for Thermoset Matrix Composites: Thermochemical Considerations," *Polym. Compos.*, **22**, 118 (2001).

Nzihou, A., P. Sharrock, and A. Ricard, "Reaction Kinetics and Heat Transfer Studies in Thermoset Resins," *Chem. Eng. J.*, **72**, 53 (1999).

Oh, J. H., and D. G. Lee, "Cure Cycle for Thick Glass/Epoxy Composite Laminates," *J. Compos. Mater.*, **36**, 19 (2002).

Olivier, P., and J. P. Cottu, "Optimisation of the Co-Curing of Two Different Composites with the Aim of Minimising Residual Curing Stress Levels," *Compos. Sci. Technol.*, **58**, 645 (1998).

Park, H. C., N. S. Goo, K. J. Min, and K. J. Yoon, "Three-Dimensional Cure Simulation of Composite Structures by the Finite Element Method," *Compos. Struct.*, **62**, 51 (2003).

Patankar, S. V., *Numerical Heat Transfer and Fluid Flow*, Hemisphere, New York (1980).

Sun, L., S. S. Pang, A. M. Sterling, I. I. Negulescu, and M. A. Stubblefield, "Dynamic Modeling of Curing Process of Epoxy Prepreg," *J. Appl. Polym. Sci.*, **86**, 1911 (2002).

Um, M. K., I. M. Daniel, and B. S. Hwang, "A Study of Cure Kinetics by the Use of Dynamic Differential Scanning Calorimetry," *Compos. Sci. Technol.*, **62**, 29 (2002).

Manuscript received Nov. 27, 2003, and revision received Mar. 15, 2004.